Quantum-confinement effect on holes in silicon nanowires: Relationship between wave function and band structure

Naoya Morioka, Hironori Yoshioka, Jun Suda, and Tsunenobu Kimoto

Citation: J. Appl. Phys. **109**, 064318 (2011); doi: 10.1063/1.3552593
View online: http://dx.doi.org/10.1063/1.3552593
View Table of Contents: http://jap.aip.org/resource/1/JAPIAU/v109/i6
Published by the American Institute of Physics.

Quantum-confinement effect on holes in silicon nanowires: Relationship between wave function and band structure

Naoya Morioka,[1,a)] Hironori Yoshioka,[1] Jun Suda,[1] and Tsunenobu Kimoto[1,2]
[1]*Department of Electronic Science and Engineering, Kyoto University, Kyoto 615-8510, Japan*
[2]*Photonics and Electronics Science and Engineering Center, Kyoto University, Kyoto 615-8510, Japan*

(Received 28 September 2010; accepted 26 December 2010; published online 28 March 2011)

The authors theoretically studied the valence band structure and hole effective mass of rectangular cross-sectional Si nanowires (NWs) with the crystal orientation of [110], [111], and [001]. The E–k dispersion and the wave function were calculated using an $sp^3d^5s^*$ tight-binding method and analyzed with the focus on the nature of p orbitals constituting the subbands. In [110] and [111] nanowires, longitudinal/transverse p orbitals are well separated and longitudinal component makes light (top) subbands and transverse component makes heavy subbands. The heavy subbands are located far below the top light band when NW has square cross-section, but they gain their energy with the increase in the NW width and come near the band edge. This energy shift of heavy bands in [110] NWs shows strong anisotropy to the direction of quantum confinement whereas that in [111] NWs does not have such anisotropy. This anisotropic behavior and the difference among orientations are understandable by the character of the wave function of heavy subbands. Regarding the [001] nanowires, the top valence state is formed by the mixture of longitudinal/transverse p orbitals, which results in heavy effective mass and large susceptibility to lateral-size variation. The correlation of the wave function of hole states between nanowires and bulk is also discussed briefly. © *2011 American Institute of Physics*. [doi:10.1063/1.3552593]

I. INTRODUCTION

Silicon nanowires (NWs) have caught a great deal of attention as a promising building block of future optoelectronic devices[1,2] and integrated circuits.[3] In particular, silicon nanowires are very attractive as a channel material for metal-oxide-semiconductor field-effect transistors (MOSFETs) because they exhibit excellent immunity to short-channel effects.[4–8] Si NW MOSFETs with the channel width down to a few nanometers have successfully been fabricated[9] and some experimental studies reported that transport performance of Si NW MOSFETs may exceed that of conventional bulk Si MOSFETs.[10,11]

In nanostructures such as quantum wells, wires, and dots, quantum-confinement effect alters electronic states, and it results in a significant change of energy band structure. Because band structure affects the characteristics of carrier transport to a great extent, sufficient understanding of the band structure of NWs is essential to predict the device performance of Si NW MOSFETs. For this reason, a number of theoretical studies have been performed thus far to investigate the influence of such quantum-confinement conditions as the wire width and orientation on the band structure.[12–20]

These theoretical studies have revealed that the major feature of conduction band structure of Si NWs dependent on the orientation and the size can be captured from the feature of the band structure of bulk Si by applying a single-band effective mass approach, especially in thick (>5 nm) wires. It is worth noting that even the electron effective mass in NWs under strong quantum confinement is understandable by full energy-wave number, $E-k$, dispersion of the conduction band of bulk crystal.[19] These facts indicate that the single-band picture can be a good approximation for electron states of Si NWs and that the interaction between equivalent six conduction-band valleys is small.

On the other hand, it is considered that simple interpretation is not available for valence band (VB) of NWs because hole states are mainly composed of three p orbital characters and these orbitals have interactions with each other. Under strong quantum confinement, this interaction mixes the light, heavy, and split-off hole states described in bulk and generates new hole states in NWs. Since the p orbitals have strong anisotropy, hole states in NWs are expected to be very sensitive to the orientation and cross-sectional structure of NWs, which makes the situation more complicated. Though a certain level of qualitative estimation from bulk band structure is available for very thick (>10 nm) NWs,[20] this straightforward prediction may not be very accurate under stronger quantum confinement. Therefore, the nature of hole states unique to NWs must be studied comprehensively.

Previous theoretical studies on valence band states of Si NWs have obtained some common results about properties of holes in Si NWs. For example, it is a commonly observed result that [001] Si NWs exhibit large hole effective mass at VB maximum (VBM) and [110] and [111] NWs show small mass.[13–15,20] This tendency is also observed in other diamond- and zinc-blende-type semiconductor NWs such as Ge,[15] InP,[21,22] and InAs.[22] However, the origin of this property is still unclear even though the physical understanding of this result is essential to discuss the transport performance of Si NWs.

In this paper, the authors attempted to understand the behavior of holes on quantum confinement in Si NWs comprehensively by theoretical calculation. Because hole states

[a)]Author to whom correspondence should be addressed. Electronic address: morioka@semicon.kuee.kyoto-u.ac.jp.

in Si NWs are strongly affected by the anisotropy of p orbitals as mentioned above, it is desirable to adopt a calculation method which can evaluate the contribution of atomic p orbitals directly. For this purpose, we employed a nearest-neighbor $sp^3d^5s^*$ tight-binding method,[23–25] which describes the VB states of semiconductors with keeping a clear view of electronic structures. To investigate the effects of quantum-confinement condition such as width, height, and orientation of NWs, the authors calculated the band structure, effective mass, and atomiclike-orbital-decomposed wave function of rectangular cross-sectional [001], [110], and [111] Si NWs with a wide range of the aspect ratio. From this calculation, it is found that the main properties of the subbands such as effective mass and quantization energy are clearly attributed to the character of atomic orbitals which constitute the state of the subband.

This paper is organized as follows. In Sec. II, the details of calculation method and the structure of NWs are described. In Sec. III, the VB structure and hole effective mass of NWs under various quantum-confinement conditions are shown. The correlation among the band structure, effective mass, and the character of wave function is presented. Section IV discusses about the physical understanding of the relationship between the property of band structure and the character of wave function. Furthermore, the correspondence between hole states in NWs and those in bulk is also discussed here. The paper is concluded in Sec. V.

II. CALCULATION DETAILS

A. Calculation method

For the calculation of electronic structures of NWs, a nearest-neighbor $sp^3d^5s^*$ tight-binding method is employed.[23–25] This method considers one s orbital, three p orbitals $\{p_x, p_y, p_z\}$, five d orbitals $\{d_{yz}, d_{zx}, d_{xy}, d_{3z^2-r^2}, d_{x^2-y^2}\}$, and one excited s^* orbital. The coordinate axes of x, y, and z are fixed to the [100], [010], and [001] directions, respectively.

The effect of spin-orbit (SO) coupling[26] is included in this study. To distinguish up-spin and down-spin states for each atomic orbital, the twice number of atomic orbitals is necessary, i.e., the orbital set becomes $\mathcal{B} = \{s, p_x, p_y, p_z, d_{yz}, d_{zx}, d_{xy}, d_{3z^2-r^2}, d_{x^2-y^2}, s^*\} \otimes \{\uparrow, \downarrow\}$. The calculation with SO coupling produces more accurate results deservingly, whereas it should be noted that the VB structure and effective mass of thin (<5 nm) NWs are not very sensitive to the SO interaction.

Surface dangling bonds were pacified by sp^3 hybridization scheme,[27] which brings a similar situation as hydrogen termination. The $sp^3d^5s^*$ parameter set of Si was taken from Ref. 25.

In a tight-binding approximation, the wave function with a wave number vector $\boldsymbol{k}$, $\Psi(\boldsymbol{k})$, is expressed as a linear combination of Bloch sums $\Phi_{\alpha m}(\boldsymbol{k})$ of atomiclike orbitals (labeled $m \in \mathcal{B}$) centered at an equivalent atom position (labeled α) over N unit cells constituting the NW:

$$\Phi_{\alpha m}(\boldsymbol{k}) = \frac{1}{\sqrt{N}} \sum_l e^{i\boldsymbol{k}\cdot(\boldsymbol{R}_\alpha + l\boldsymbol{T})} \phi_m(\boldsymbol{r} - \boldsymbol{R}_\alpha - l\boldsymbol{T}), \quad (1)$$

$$\Psi(\boldsymbol{k}) = \sum_\alpha \sum_m c_{\alpha m}(\boldsymbol{k}) \Phi_{\alpha m}(\boldsymbol{k}), \quad (2)$$

where ϕ_m is the wave function of Si's Löwdin orbital[28] of m, $\boldsymbol{R}_\alpha$ is a direct vector to the Si atom labeled α, $\boldsymbol{T}$ is the translation vector of the NW crystal. By diagonalizing the tight-binding Hamiltonian matrix at a given $\boldsymbol{k}$, energy levels, E, and superposition coefficient of each Bloch sum, $[c_{\alpha m}]$, are obtained as eigenvalues and eigenvectors, respectively. From the obtained coefficient vector corresponding to the certain state, we define the degree of contribution of atomic orbitals, which represents how much the orbital is involved in this state. For example, the degree of contribution from the p_x orbital is defined by $\sum_\alpha \sum_{\sigma=\uparrow,\downarrow} |c_{\alpha p_x^\sigma}|^2$, where p_x^σ indicates the p_x orbital with the spin state of σ. The cases of the other orbitals are defined in the same way. By calculating the contribution of each orbital, we investigated the relationship between the character of wave function and properties of the VB structure. It is a great strength of a tight-binding method that these analysis can be performed straightforward.

B. Nanowire structures

To capture the effects of quantum confinement, square and rectangular cross-sectional Si NWs were calculated in this study. The results of rectangular cross-section give us information about the anisotropy of quantization effect by different surfaces. The axial orientation and two side faces were determined as $[001]/(100)/(010)$, $[110]/(001)/(1\bar{1}0)$, and $[111]/(11\bar{2})/(\bar{1}10)$. The detailed crystal structures and geometry settings are illustrated by ball-stick images in Fig. 1. In the square case, the height and width were varied from 1 to 13 nm. In the rectangular case, the height was kept constant at 2.0 nm (for the height along $\langle 001 \rangle$ and $\langle 11\bar{2} \rangle$) or 1.9 nm (for along $\langle 1\bar{1}0 \rangle$) while the width was varied from 1 to 13 nm. The width and height are determined by the distance between the center of atoms at both ends. The space group of each geometry of NW crystal is described in Table I.

In our calculation, the effect of strain, relaxation, and surface reconstruction were neglected because our interest in this paper is the understanding of quantum-confinement effects on holes. Therefore, the bonds between Si atoms were assumed to be ideal sp^3 bonds, and the bond length was set at 2.352 Å, the same value as in bulk Si [the lattice constant of bulk Si is $a_0 = 5.431$ Å (Ref. 29)].

III. CALCULATION RESULTS

A. [001] nanowires

In an $sp^3d^5s^*$ tight-binding method, the state space of VBM of bulk Si (heavy, light, and split-off holes) is built by the orbital set of $\{p_x, p_y, p_z, d_{yz}, d_{zx}, d_{xy}\} \otimes \{\uparrow, \downarrow\}$.[25] We found that this result holds true in NWs because the incorporation of s, d_{3z^2-r-2}, $d_{x^2-y^2}$, and s^* components by quantum confinement is very small. Therefore, the degree of contribution is calculated only for these six characters of p and d orbitals. To emphasize the fact that the directionality of these orbitals is along the three axes of NWs' geometry ($[100]/[010]/[001]$), we rewrite $p_x, p_y, p_z, d_{yz}, d_{zx}$, and d_{xy} as $p_{100}, p_{010}, p_{001}, d_{100}, d_{010}$, and d_{001}, respectively. In addition we put p_{lmn} and d_{lmn} into the single denotation $|lmn)$ because

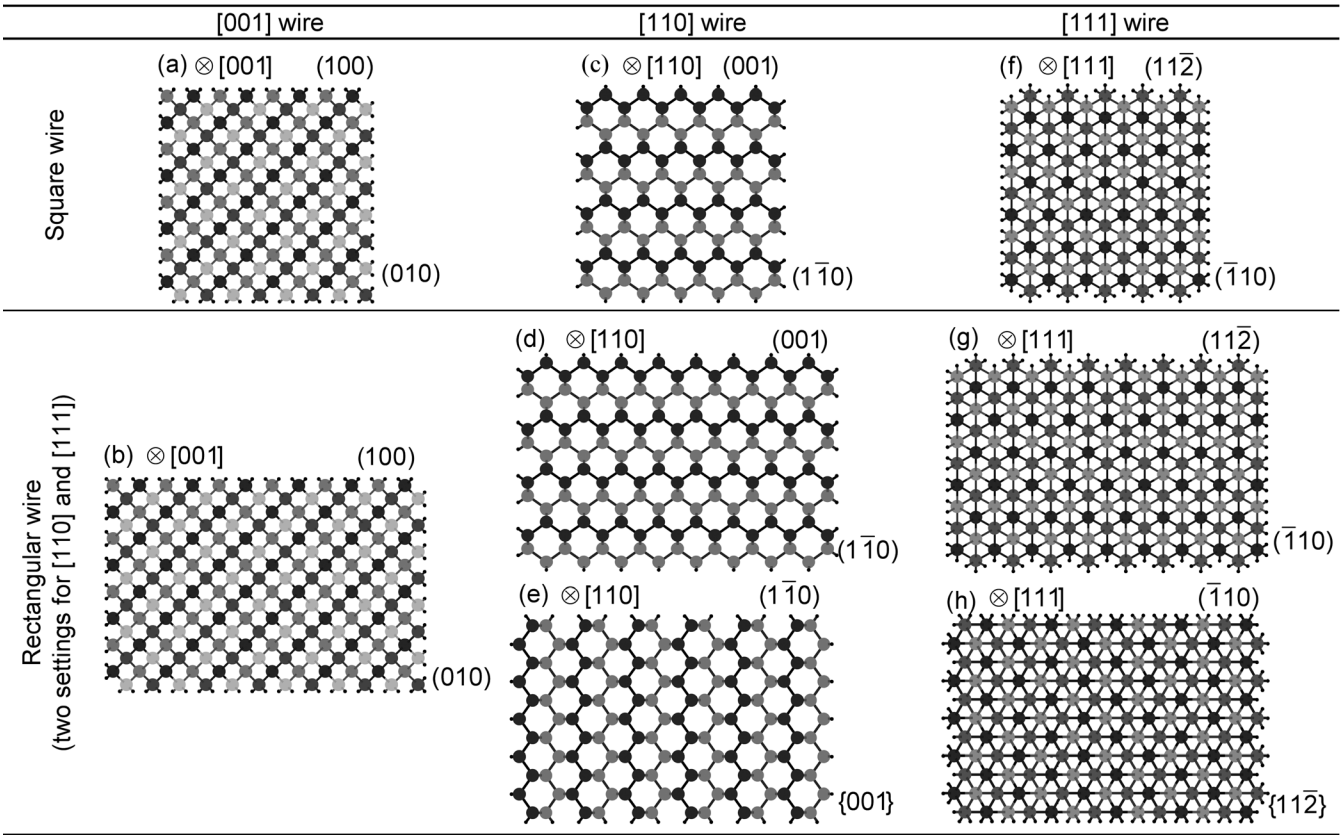

FIG. 1. Ball-stick structures of calculated silicon nanowires. This figure illustrates nanowires with the height of approximately 2 nm. Surface bonds with small black balls indicate the passivated sp^3 bonds. Each figure illustrates (a) [001] square, (b) [001] rectangular, (c) [110] square, (d) [110]/(001) rectangular, (e) [110]/(1$\bar{1}$0) rectangular, (f) [111] square, (g) [111]/(11$\bar{2}$) rectangular, and (h) [111]/($\bar{1}$10) rectangular nanowires.

they are classified into the same symmetry character when they are arranged in a diamond-type lattice.

Figure 2 shows the hole effective mass and contribution of each atomic orbital at VBM in square cross-sectional [001] Si NWs as a function of the width. Hole effective mass of [001] NWs takes a minimum at a width of 2 nm and increases as the width departs from the maximum point. The contribution of atomic orbitals exhibits a characteristic change responding to the change in the effective mass. It is clearly observed that the p_{001} orbital, which is the main component of the VB top, makes a maximum contribution when the effective mass becomes minimum and its fraction decreases as the effective mass increases. The width dependence of composition of the d_{001} orbital, whose symmetry character is the same as p_{001}, is similar to that of p_{001}, whereas the magnitude of contribution from d_{001} is less than about a fifth of that from p_{001}. From this result, one may say that $|001)$ is actually the p_{001} orbital. This holds also true for $|100)$, $|010)$, and other orbital characters of $|lmn)$ defined for [110] and [111] wires later in this paper. The degree of contribution from p_{100} and p_{010} orbitals exhibits the minimum at the minimum point of the effective mass and increases with the increase in the effective mass, which is an opposite change to the case of the p_{001} orbital. In summary, a hole state with a larger fraction of p orbital along the transport direction and smaller along the confinement direction exhibits smaller effective mass.

TABLE I. Space group of calculated nanowire crystals.

	Square	Rectangular
[001]	$P2/m$	$P\bar{1}$
[110]	$Pmma$	$Pmma$
[111]	$P2/m$	$P2/m$

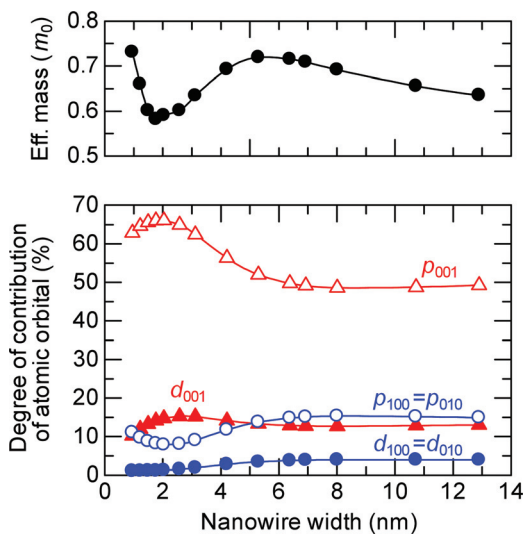

FIG. 2. (Color online) Hole effective mass and degree of contribution of atomic orbitals (at the valence band top) in square cross-sectional [001] silicon nanowires.

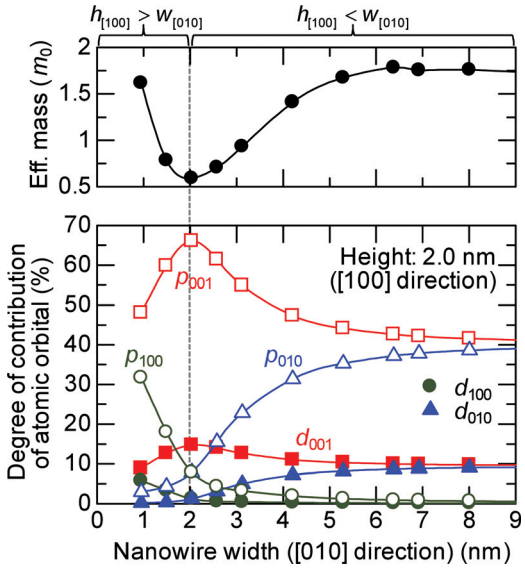

FIG. 3. (Color online) Hole effective mass and degree of contribution of atomic orbitals (at the valence band top) in rectangular cross-sectional [001] silicon nanowires. The height ($h_{[100]}$) is kept at 2.0 nm and the width ($w_{[010]}$) is varied.

Figure 3 shows the width dependence of hole effective mass and degree of contribution of p and d orbitals at the VB top in rectangular [001] Si NWs. The height of nanowires ($h_{[100]}$) is kept at 2.0 nm and the width ($w_{[010]}$) is variable. It is clearly observed that the effective mass takes minimum when the nanowire has a square cross section and becomes heavier rapidly when $w_{[010]}$ increases or decreases from 2.0 nm. This increase in the effective mass is easily understood from the variation of energy dispersion (Fig. 4). Only in the square case, the dispersion curve has a 'small hill' at VBM, which gives smaller effective mass in square wires. However, the energy range of this small hill is mere approximately 30 meV and thus the inherent nature of the top subband is considered as the band with heavy effective mass.

In rectangular NWs, the contribution from p_{001} exhibits maximum in the square case and decreases with the increase in the effective mass when the width is varied. This correspondence between the effective mass and the degree of contribution from p_{001} is the same as the case in square NWs. In addition, the contribution from p_{100} and p_{010} changes significantly by the change of the width in rectangular NWs. First, in the case of $h_{[100]} = w_{[010]}$, the contribution from the p_{100} and p_{010} orbitals is equal. However, in the case of $h_{[100]} < w_{[010]}$, the contribution from the p orbital along the width direction (p_{010}) increases and that from the p orbital along the height direction (p_{100}) decreases, and vice versa in the case of $h_{[100]} > w_{[010]}$. In other words, the p orbital parallel to the wider surface mixes into the VBM state with large amount in rectangular cross-sectional NWs, and thus the fraction of p_{001} decreases. Although above results are obtained for very thin (2.0 nm) nanowire, we also observed similar results for 4.2-nm-height [001] NWs.

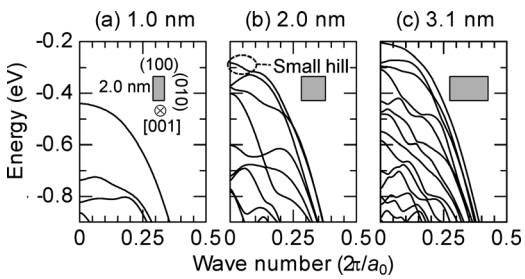

FIG. 4. Valence band structure of 2.0-nm-height rectangular cross-sectional [001] nanowires, where the width is (a) 1.0 nm, (b) 2.0 nm, and (c) 3.1 nm. The energy is referenced from the band edge of bulk. Inset rectangles indicate the cross-sectional shape of calculated nanowires.

B. [110] nanowires

In respect to $[110]/(001)/(1\bar{1}0)$ NWs, the p_x and p_y orbitals are unsuitable basis for atomic orbital analyses because they swap each other by symmetry operations which the crystal has. Hence we used p_{110} and $p_{1\bar{1}0}$ as the basis for p orbital analyses, where p_{110} and $p_{1\bar{1}0}$ are p orbitals along the [110] (transport) direction and the $[1\bar{1}0]$ (width or height) direction, respectively. These orbitals can be obtained by

$$p_{110} = (p_x + p_y)/\sqrt{2},$$
$$p_{1\bar{1}0} = (p_x - p_y)/\sqrt{2},$$

and for d orbitals d_{110} and $d_{1\bar{1}0}$ are similarly defined by

$$d_{110} = (d_{yz} + d_{zx})/\sqrt{2},$$
$$d_{1\bar{1}0} = (d_{yz} - d_{zx})/\sqrt{2}.$$

These four orbitals plus $p_{001} = p_z$ and $d_{001} = d_{xy}$ form the orthonormal basis set for atomic orbital analyses. In practice, after constructing and diagonalizing the Hamiltonian matrix in the regular basis $\mathcal{B}$, unitary transform was performed into new basis set, and the degree of contribution was calculated.

Figure 5 describes the width dependence of hole effective mass and contribution of each atomic orbital at VBM in square [110] Si NWs. The light-hole effective mass of bulk Si calculated by the same tight-binding method (w/ and w/o SO coupling) is also plotted in the figure. It is found that

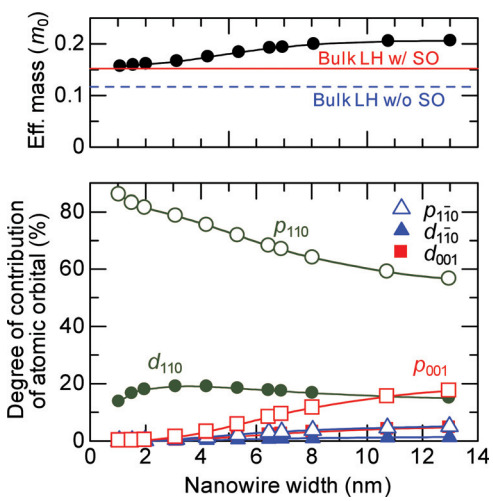

FIG. 5. (Color online) Hole effective mass and degree of contribution of atomic orbitals (at the valence band top) in square cross-sectional [110] silicon nanowires.

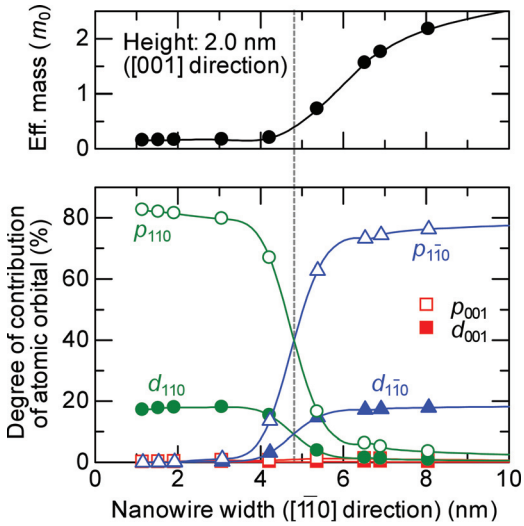

FIG. 6. (Color online) Hole effective mass and degree of contribution of atomic orbitals (at the valence band top) in rectangular cross-sectional [110]/(001) silicon nanowires. The height along [001] is kept at 2.0 nm and the width along [1$\bar{1}$0] is varied.

[110] NWs exhibit small effective mass close to that of bulk's light hole. In addition, the effective mass obtained in our calculation shows good agreement with first-principles calculations.[13,14] From wave function analyses, it is revealed that the hole state at VBM in square NWs is well described by p_{110}, which is parallel to the transport direction.

Next, the results of rectangular wires are described. There are two settings of geometry for rectangular cross-sectional [110] NWs: [110]/(001) [Fig. 1(d)] and [110]/(1$\bar{1}$0) [Fig. 1(e)]. The width dependence of hole effective mass and the degree of contribution of atomic orbitals at VBM in 2.0-nm-height rectangular [110]/(001) Si NWs is plotted in Fig. 6. In the [110]/(001) geometry, the height and width directions are along [001] ($h_{[001]}$) and [1$\bar{1}$0] ($w_{[1\bar{1}0]}$), respectively. In the case $w_{[1\bar{1}0]} < 4$ nm, the effective mass is as small as that in square [110] wires. In the case $w_{[1\bar{1}0]} < 4$ nm, however, the effective mass of the top subband increases with the width. The orbital analysis reveals that this variation of effective mass by the variation of $w_{[1\bar{1}0]}$ accompanies the variation of the main character of wave function from $|110)$ to $|1\bar{1}0)$.

This change of the effective mass and the character of wave function is due to the change in ordering of subbands that have different characteristics. Calculated band structure of 2.0-nm-height rectangular [110]/(001) Si NWs is shown in Fig. 7. The band structure of [110] NWs contains three different types of subbands — one with small effective mass (L band), another with large effective mass (H band), and the third with a shape like the right half of 'M' letter (M band). When $w_{[1\bar{1}0]} < 4$ nm, the L band forms the VB top and the H band is located far below the top L band. The H band, however, increases its energy as the width increases and finally comes over the top L band, which results in the increase in effective mass at VBM. From atomic orbital analyses and the band structure, the character of the L and H bands is identified as $|110)$ and $|1\bar{1}0)$, respectively. We performed additional wave function calculation for lower-energy states and

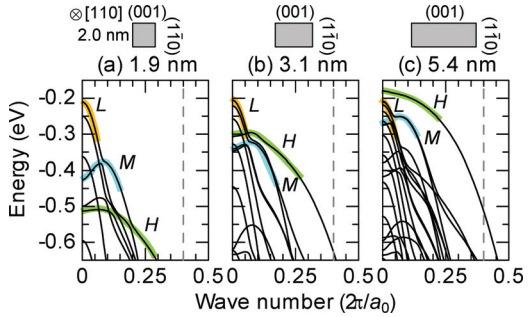

FIG. 7. (Color online) Valence band structure of 2.0-nm-height rectangular cross-sectional [110]/(001) nanowires with widths of (a) 1.9 nm (square case), (b) 3.1 nm, and (c) 5.4 nm. The energy is referenced from the band edge of bulk. Rectangles above each plot indicates the cross-sectional shape of calculated nanowires. Band structure contains three different types of subbands: small effective mass subband (L band), half-M-shaped subband (M band), and large effective mass subband (H band). The dash line indicates the position of $k = 0.4 \times 2\pi/a_0$.

confirmed that the M band has a character of $|001)$. In fact, the formation of L, M, and H bands in [110] NWs is commonly observed by many theoretical calculations of not only Si NWs (Refs. 13, 14, 20, 30–33) but also other diamond- and zinc blende-type semiconductor NWs such as Ge (Refs. 34 and 35) and InP (Ref. 21). Of these studies, Leu *et al.*[31] conducted atomic orbital analyses and identified that the main component of the L and M band states is the p orbital with a character of p_{110} and p_{001}, respectively, by density functional theory. This agrees with our tight-binding results.

On the other hand, the situation is different in [110]/(1$\bar{1}$0) rectangular wires. In 1.9-nm-thick [110]/(1$\bar{1}$0) NWs with a width of 1–13 nm ($w_{[001]}$), the L band forms the topmost band at VBM and thus both hole effective mass and the mixture fraction of atomic orbitals almost maintain the value obtained in the 2.0 nm square [110] wire. In addition, it is found that the energy of the H band is insensitive to the variation of $w_{[001]}$. The energy level of the topmost H band at $k = 0.4 \times (2\pi/a_0)$ in both 1.9-nm-thick [110]/(1$\bar{1}$0) NWs and 2.0-nm-thick [110]/(001) NWs are plotted as a function of the width ($w_{[001]}$ or $w_{[1\bar{1}0]}$) in Fig. 8. The energy level of H band is strongly dependent on the strength of [1$\bar{1}$0] confinement but less susceptible to [001] confinement. The origin of this anisotropic nature of the H band will be discussed in Sec. IV A.

Here it should be noted that the results for [110]/(001) NWs do not necessarily imply that the H band has always higher energy in sufficiently wide [110]/(001) wires. Actually,

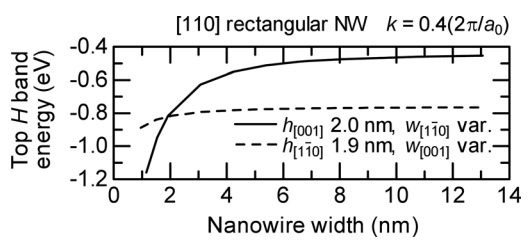

FIG. 8. The energy level of the highest heavy (H) band in [110] rectangular cross-sectional silicon nanowires at $k = 0.4 \times 2\pi/a_0$. The energy is referenced from the band edge of bulk. Solid: [110]/(001) wires with constant [001] height ($h_{[001]} = 2.0$ nm) and varying [1$\bar{1}$0] widths ($w_{[1\bar{1}0]}$); dashed: [110]/(1$\bar{1}$0) wires with constant [1$\bar{1}$0] height ($h_{[1\bar{1}0]} = 1.9$ nm) and varying [001] widths ($w_{[001]}$).

the band ordering depends on the NWs' height and the detailed crystal symmetry, and there are some cases that the energy of the H band does not exceed that of the L band. However, in those cases, the difference of the energy level between the L and H bands is very small and comparable to the thermal energy at room temperature. What is essential is that the energy level of the L and H bands can become very close and the both bands may involve to the hole transport.

C. [111] nanowires

For [111] NWs, the set of p_x, p_y, p_z, and corresponding d orbitals are unsuitable for the basis of atomic orbital analyses. Thus, we determined new p and d orbitals as $\{p_{111}, p_{11\bar{2}}, p_{\bar{1}10}, d_{111}, d_{11\bar{2}}, d_{\bar{1}10}\}$, whose directionality is along three axes of the NWs' geometry (length, height, and width direction). This orthonormal basis set for atomic orbital analyses can be obtained by following unitary transform:

$$
\begin{aligned}
p_{111} &= (p_x + p_y + p_z)/\sqrt{3}, \\
p_{11\bar{2}} &= (p_x + p_y - 2p_z)/\sqrt{6}, \\
p_{\bar{1}10} &= (-p_x + p_y)/\sqrt{2}, \\
d_{111} &= (d_{yz} + d_{zx} + d_{xy})/\sqrt{3}, \\
d_{11\bar{2}} &= (d_{yz} + d_{zx} - 2d_{xy})/\sqrt{6}, \\
d_{\bar{1}10} &= (-d_{yz} + d_{zx})/\sqrt{2}.
\end{aligned}
$$

Figure 9 shows the width dependence of hole effective mass and contribution of each atomic orbital at VBM in square cross-sectional [111] Si NWs. The effective mass of [111] NWs is very small and very close to that of bulk light hole, and the wave function of the topmost subband at the Γ point is almost pure state of $|111)$, which is directed to the transport orientation. The effective masses of [111] Si NWs obtained by our calculation well agree with those by other theoretical studies.[13,14,36] The band structure of square [111] Si NWs appears in Fig. 10. It is clearly observed that upper subbands around the zone center generally have small effective mass (L' band), and upper subbands distant from the zone center have large effective mass (H' band). To investigate the character of wave function of an H' subband, atomic orbital analyses were performed for the H' state with the highest energy at $k = 0.2 \times 2\pi/a_0$, and the result for square NWs is shown in Fig. 11(a). As the plot indicates, H' subbands are formed by orbitals along confinement directions, the mixture of $|11\bar{2})$ and $|\bar{1}10)$. Leu *et al.*[31] have found by a first-principles calculation that the top heavy band in hexagonal cross-sectional [111] Si NWs have pure character of $p_{\bar{1}10}$, not a mixture of $p_{\bar{1}10}$ and $p_{11\bar{2}}$. This discrepancy may be due to the difference of cross-sectional shape and symmetry. We should mention that the general shape of the band structure of [111] nanowires is common in diamond- and zinc-blende-type semiconductors such as Si (Refs. 13, 14, 20, 31, 36), Ge Refs. 34, 36), InP (Ref. 21), and GaAs (Ref. 37). In particular, Ref. 37 states about GaAs NWs that the wave function of the states with small effective mass have its characteristic extension along the transport direction and that with large effective mass have extension in the transverse direction. This observation is consistent with our results.

We calculated the band structure and effective mass of rectangular cross-sectional $[111]/(11\bar{2})$ (2.0-nm-height) and $[111]/(\bar{1}10)$ (1.9-nm-height) wires by varying a width from 1 to 13 nm. From this calculation, we found that in every case the L' subband appeared as the top band at the zone center and as a result the effective mass at the VBM was almost constant. In addition, the energy level of the H' bands increases as the width increases though the height is kept constant, but the energy of the H' band does not exceed that of the L' band. The amount of the energy shift is almost isotropic (see Fig. 12, which describes the energy level of the top H' band at $k = 0.2 \times 2\pi/a_0$ in the both rectangular structures). This feature of H' band in [111] NWs is quite different from that of H band in [110] NWs.

The orbital analysis for rectangular wires revealed that the top L' subband remained almost pure $|111)$ state but that the composition of the orbital of the top H' band was dependent on the geometry of NWs. Figures 11(b) and 11(c) show the width dependence of the composition of atomic orbitals of the topmost H' subband at $k = 0.2 \times 2\pi/a_0$ in rectangular [111] wires. In square cross-sectional wires, the top H' band is composed of the mixture of $|11\bar{2})$ and $|\bar{1}10)$, as discussed

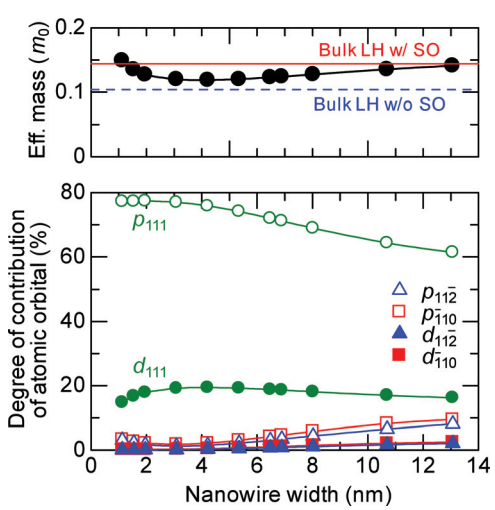

FIG. 9. (Color online) Hole effective mass and degree of contribution of atomic orbitals (at the valence band top) in square cross-sectional [111] silicon nanowires.

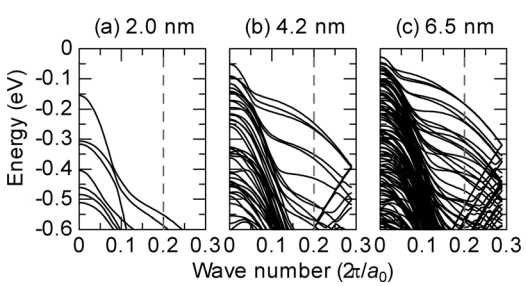

FIG. 10. Valence band structure of square cross-sectional [111] silicon nanowires, where the width is (a) 2.0 nm, (b) 4.2 nm, and (c) 6.5 nm. The energy is referenced from the band edge of bulk. The boundaries of the first Brillouin zone are located at $\pm 2\pi/\sqrt{12}a_0$. The dash line indicates the position of $k = 0.2 \times 2\pi/a_0$.

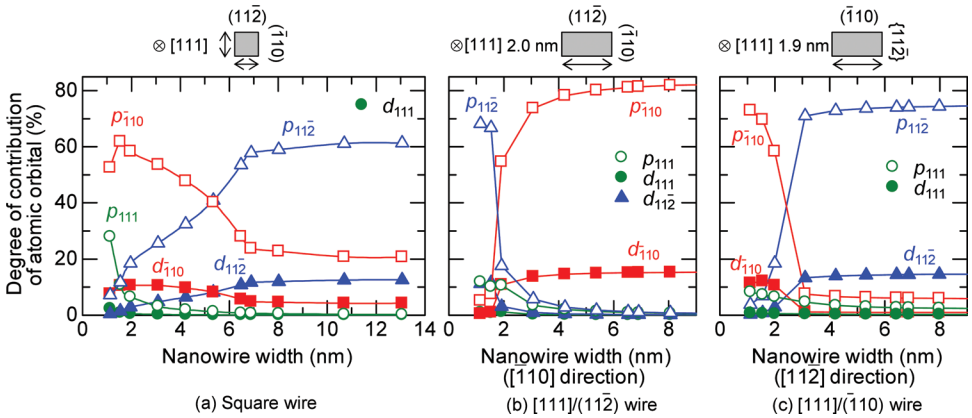

FIG. 11. (Color online) Degree of atomic orbital contribution of topmost hole state at $k = 0.2 \times 2\pi/a_0$ in (a) square cross-sectional [111], (b) 2.0-nm-height rectangular cross-sectional $[111]/(11\bar{2})$, and (c) 1.9-nm-height rectangular cross-sectional $[111]/(\bar{1}10)$ silicon nanowires.

above. In rectangular wires, however, the mixing of $|11\bar{2})$ and $|\bar{1}10)$ is dissolved and the top heavy subband is formed by almost single character of $\{p, d\}$ orbitals along the direction of the wider thickness. Here let us take 2-nm-height $[111]/(11\bar{2})$ NWs as an example [see Fig. 11(b)]. When the width (along $[\bar{1}10]$) is larger than the height (along $[11\bar{2}]$), the topmost H' subband becomes almost pure $|\bar{1}10)$ state. We should emphasize that this result does not say that H' subbands with single $|11\bar{2})$ character and the mixed state of $|11\bar{2})$ and $|\bar{1}10)$ disappeared. These states form other lower-energy H' subbands existing below the top $|\bar{1}10)$ band.

IV. DISCUSSION

A. Transport effective mass vs character of atomic orbital

First, we will discuss about the transport effective mass in NWs. In Sec. III, we found that a subband with large amount of p component oriented to the transport direction has small transport effective mass and one with large contribution from p orbital perpendicular to the transport direction has large transport effective mass, which is a common result to [001], [110], and [111] wires. This result is not hard to be understood instinctively, but in regard to [110] and [111] wires this result is comprehensible more deeply by checking the overlap of orbitals between neighbor atoms.

Figures 13(a)–13(c) show how three p orbitals arrange at each atom position in [110] NWs. Each p orbital is drawn by the combination of black and white balls, where the shape describes the symmetry of the orbital and the contrast denotes the phase. Note that the phase of the p orbital is opposite between nearest neighbor atoms. The thickness of bonds between neighbor atoms and the size of orbitals described in these figures are changed by considering perspective; the thicker bond denotes the bond on the nearer side, and the thinner on the farther (the size of orbitals is likewise). In [110] NWs, p_{110} orbitals form strong σ-bonding state toward the transport direction, which results in large overlap of orbitals along the transport direction. On the other hand, $p_{1\bar{1}0}$ orbitals make complete π-antibonding state along [110], and thus the overlap of orbitals toward the transport direction is extremely small. These properties of p_{110} and $p_{1\bar{1}0}$ orbitals agree with the calculation results that the L band ($|110)$ character) has very small transport effective mass and the H band ($|1\bar{1}0)$ character) has very large mass.

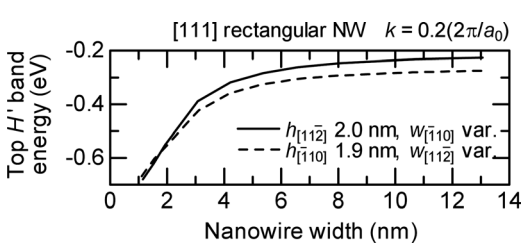

FIG. 12. The energy level of the highest heavy (H') band in [111] rectangular cross-sectional silicon nanowires at $k = 0.2 \times 2\pi/a_0$. The energy is referenced from the band edge of bulk. Solid: $[111]/(11\bar{2})$ wires with constant $[11\bar{2}]$ height ($h_{[11\bar{2}]} = 2.0$ nm) and varying $[\bar{1}10]$ widths ($w_{[\bar{1}10]}$); dashed: $[111]/(\bar{1}10)$ wires with constant $[\bar{1}10]$ height ($h_{[\bar{1}10]} = 1.9$ nm) and varying $[11\bar{2}]$ widths ($w_{[11\bar{2}]}$).

Similar argument is applicable for [111] NWs. The arrangement of three p orbitals at each atom position in [111] NWs is shown in Figs. 13(d)–13(f). The p_{111} orbital, which corresponds to subbands with small effective mass, forms large overlap of orbitals toward the transport direction. On the other hand, the $p_{11\bar{2}}$ and $p_{\bar{1}10}$ orbitals, which correspond to subbands with large effective mass, form small overlap of orbitals due to π-antibonding arrangement toward the [111] direction.

Here we give a brief discussion about the relationship of character of wave function between bulk and NWs. Our calculation presented thus far includes the effect of SO coupling, but we also performed the calculation without SO coupling and confirmed that the general shape of the band structure and the effective mass of [110] and [111] wires are not very sensitive to SO coupling. Therefore, it is reasonable to suppose that SO coupling is not of importance to determine the electronic property of Si NWs. This insensitivity to SO coupling is due to the relatively small SO splitting energy of silicon (0.045 eV in experimental, 0.047 eV in the $sp^3d^5s^*$ tight-binding fitting) compared to the quantum-confinement energy. The analytical formulas of effective mass and wave function of holes along [001], [110], and [111] in bulk Si by $sp^3d^5s^*$-SO model have been shown by Boykin *et al.*[25] However, the direct comparison between the wave function components of NWs and $sp^3d^5s^*$-SO bulk does not work well

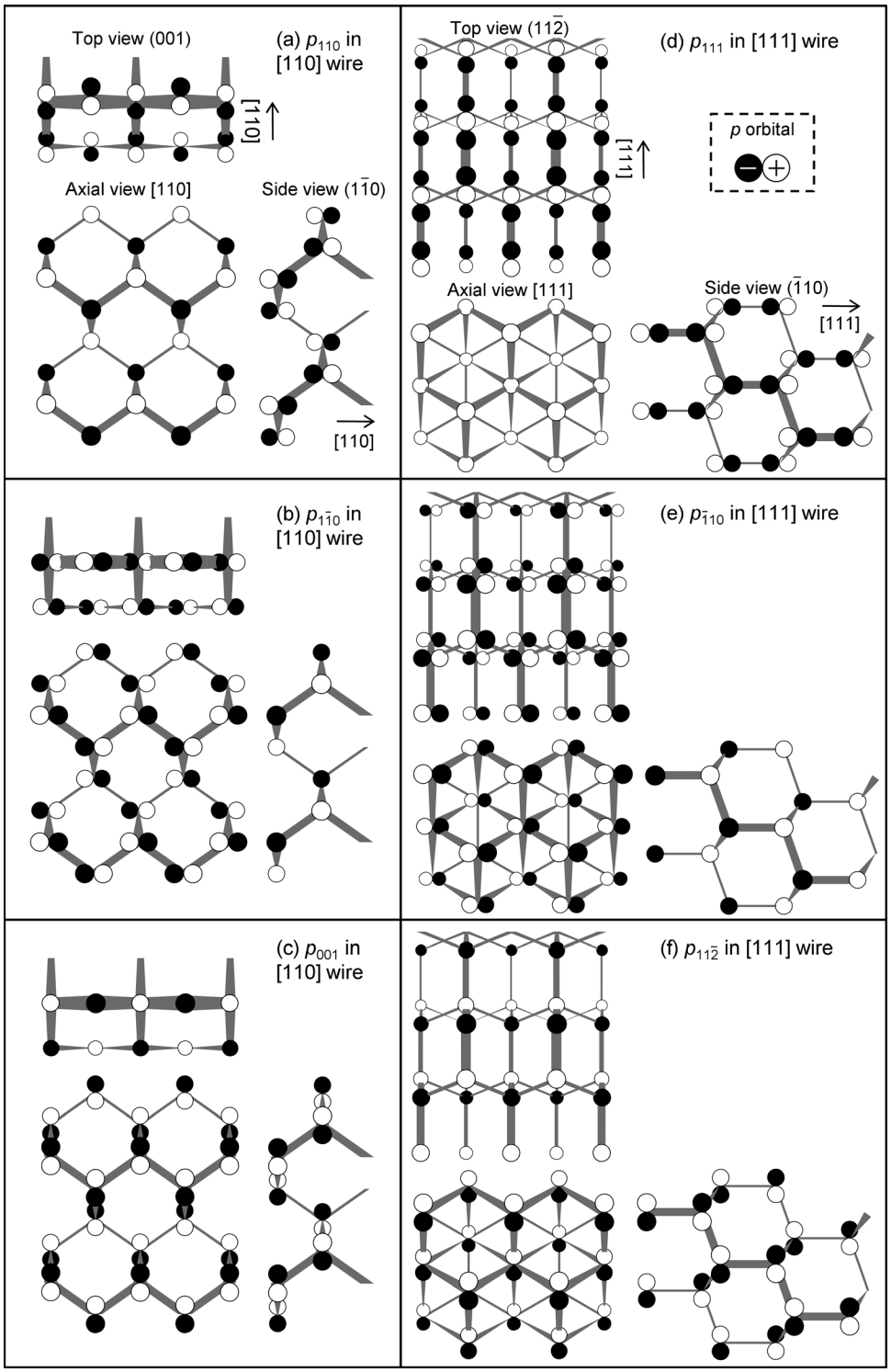

FIG. 13. Schematic image of arrangement of p orbital in [110] and [111] nanowires: (a) p_{110} in [110] nanowires, (b) $p_{1\bar{1}0}$ in [110] nanowires, (c) p_{001} in [110] nanowires, (d) p_{111} in [111] nanowires, (e) $p_{\bar{1}10}$ in [111] nanowires, and (f) $p_{11\bar{2}}$ in [111] nanowires. Each figure includes axial, top, and side views. The thickness of bonds between neighbor atoms and the size of orbitals are changed by considering perspective. The contrast of p orbitals (white/black) indicates the phase of the function.

because the bulk model with SO treats heavy/light and split-off holes as separated off. The SO coupling effect is less important in NW due to the strong geometric (or electric) confinement, and thus the comparison with the bulk model without SO, which treats three p states equivalently, is more meaningful. The wave function of hole states along [001], [110], and [111] by $sp^3d^5s^*$ tight-binding without SO can be derived by employing the powerful method of Refs. 25 and 38. However, for simplicity, we use Dresselhaus-Kip-Kittel (DKK) 3 band $\boldsymbol{k}\cdot\boldsymbol{p}$ theory for discussion of bulk states.[39] Note that 3 band DKK theory and tight-binding without SO give the wave functions of holes with the same properties.

In DKK theory, the wave function of [110] light hole ($\boldsymbol{k}=(k,k,0)/\sqrt{2}$) is described as $|\mathrm{LH};[110]\rangle \sim (|X\rangle + |Y\rangle)$ and that of [111] light hole ($\boldsymbol{k}=(k,k,k)/\sqrt{3}$) is described as $|\mathrm{LH};[111]\rangle \sim (|X\rangle + |Y\rangle + |Z\rangle)$, where $|X\rangle$, $|Y\rangle$, and $|Z\rangle$ are basis functions corresponding to $|100)$, $|010)$, and $|001)$, respectively. This means that $|\mathrm{LH};[110]\rangle$ and $|\mathrm{LH};[111]\rangle$ of bulk are described by $|110)$ and $|111)$, respectively. These characters of bulk light hole are consistent with the

characters of the L band in [110] wires and the L' band in [111] wires. In fact, we should point out that the obtained effective mass of the top L and L' band is close to that of bulk light hole as shown in Figs. 5 and 9. Also in GaAs nanowires, it has been reported that the hole effective mass of light subband in [111] wires is very close to that of bulk light hole of GaAs.[37] Therefore, these light subbands in [110] and [111] NWs might have roots in the light-hole state in bulk Si. It is also worth mentioning that eigenstates of bulk heavy hole along the [110] direction and [111] direction are described by DKK theory as $\{|X\rangle - |Y\rangle\}$ and $\{|X\rangle + |Y\rangle - 2|Z\rangle, -|X\rangle + |Y\rangle\}$, respectively, where the [110] heavy hole is for the heaviest band and the [111] is for the doubly degenerate heavy band. In response to this, the heavy band in [110] and [111] NWs is formed by the orbital $\{|1\bar{1}0\rangle\}$ and $\{|11\bar{2}\rangle, |\bar{1}10\rangle\}$, respectively. This indicates the heavy band in nanowires along these two directions may stem from heavy-hole state of bulk.

Unlike [110] and [111] wires, the situation is complicated for [001] NWs because longitudinal and transverse component of atomic orbitals are strongly coupled. Why three states are strongly coupled and how these states are described are open to discussion and further study is necessary. However, one may say that this longitudinal-transverse orbital coupling in [001] NWs leads to large effective mass compared to [110] and [111] NWs because the transport effective mass is much affected by the mixture fraction of transverse p component. In addition, transport effective mass of [001] NWs is very sensitive to the variation of the width and height. This may be also attributed to the mixed character of p orbitals constituting the top band.

We have intensively discussed on the basis of the characters of p orbitals, but as mentioned in Ref. 25 the interactions between p and other orbitals would be also important in the framework of the tight-binding method. Therefore, further investigation from this standpoint in nanowires is required.

B. Energy shift by quantum confinement vs character of atomic orbital

Next, we consider the shift of energy levels by quantum confinement. Neophytou *et al.* have pointed out that the energy levels of subbands with large effective mass in both [110] and [111] wires are more susceptible to the variation of the dimension than that of subbands with small effective mass.[30,40] They explain that this difference of quantization energy is due to the anisotropy of the bulk heavy-hole $E-\boldsymbol{k}$ dispersion. However, we can explain this phenomenon from a viewpoint of the character of wave function.

In [110] NWs, p_{110} forms large overlap of orbitals toward the transport direction, but it forms small overlap toward the confinement direction. In particular, the overlap along the $[1\bar{1}0]$ direction is extremely small because the bonds toward this direction have π-antibonding character. On the other hand, $p_{1\bar{1}0}$ has very large overlap along the $[1\bar{1}0]$ direction to the same extent as p_{110} has along [110]. As the relationship between the transport effective mass and the magnitude of overlap of orbitals indicates, it is expected that the larger overlap of orbitals toward the confinement direction results in the smaller confinement effective mass. In other words, the energy level of a subband with larger overlap of orbitals along the confinement direction shifts more easily by quantum confinement. As a result, the energy level of $|110\rangle$ states (L band) is insensitive to $[1\bar{1}0]$ confinement but that of $|1\bar{1}0\rangle$ states (H band) is very sensitive to $[1\bar{1}0]$ confinement. For [001] confinement, it is expected from the inspection of orbitals' arrangement that $|110\rangle$ states and $|1\bar{1}0\rangle$ states are comparable in the amount of energy shift because the arrangement and overlap of p_{110} orbital and $p_{1\bar{1}0}$ orbital looks equivalent along the [001] direction. In practice, it is not exactly simple and the amount of energy shift may become slightly different. However, we can say that the amount of energy shift by [001] confinement is expected to be small for both L and H subbands because π-antibonding bonds are involved along the [001] direction. Thus the energy shift of the L band is less susceptible to the strength of both $[1\bar{1}0]$ and [001] confinement and that of the H band has strong anisotropy, that is, the amount of the shift is expected to be large for $[1\bar{1}0]$ confinement but small for [001] confinement.

It follows from what has been discussed thus far that the difference of quantum-confinement-induced energy shift between the L subband and H subband is expected to be dominated by $[1\bar{1}0]$ confinement. In square (or circular) cross-sectional NWs, the L subband has smaller negative energy shift than the H subband, and thus the L subband comes to VBM. In rectangular $[110]/(1\bar{1}0)$ wires with a constant height of 1.9 nm, a large amount of the energy shift is introduced to the H band by strong $[1\bar{1}0]$ confinement but the shift of the L band induced by both side faces is very small. For this reason, the energy of the H subband is far below the L subband and the topmost subband always becomes the L subband, as mentioned in Sec. III B. For rectangular $[110]/(001)$ wires with a varying $[1\bar{1}0]$-oriented width, the energy position of the L band hardly varies by the variation of $(1\bar{1}0)$ thickness, but that of the H band easily moves (see Figs. 7 and 8). In the situation that the $(1\bar{1}0)$ thickness become sufficiently wide, the interchange of energy levels between the L and H bands occurs if [001]-confinement-induced energy shift of H band is smaller than that of L band. This is the case observed in calculation of 2.0-nm-thick $[110]/(001)$ Si NWs. Again we should stress that whether this interchange occurs or not depends on the calculation condition such as the thickness and detailed arrangement of atoms, and therefore the interchange itself is not an essential issue. What is important is that the energy level of the top L band and H band can become very close in rectangular $[110]/(001)$ wires but cannot in $[110]/(1\bar{1}0)$ wires due to the anisotropic behavior of the H band.

Similar discussions hold validity for [111] NWs. In square cross-sectional [111] NWs, we can recognize that p_{111} exhibits small overlap toward the confinement direction and $\{p_{11\bar{2}}, p_{\bar{1}10}\}$ does large. This indicates that the energy level of $|111\rangle$ states (L' band) is smaller than that of $\{|11\bar{2}\rangle, |\bar{1}10\rangle\}$ states (H' band). This is what is observed in Ref. 40 and why the L' band dominates around the VB top in thin NWs. The nearly isotropic energy shift due to both $[11\bar{2}]$ and $[\bar{1}10]$ confinement may originate from the fact that the H' band is formed by both $p_{11\bar{2}}$ and $p_{\bar{1}10}$. When the aspect ratio is about

unity, the both orbitals couple and form the top H' band (this coupling may be due to double degeneracy of the heavy hole states along the [111] direction in bulk Si). However, when the width is larger than the height, the coupling is dissolved and the orbital parallel to the width direction forms the top H' band because that orbital has large orbital overlap along the width direction.

Although the hole states of [001] NWs are complex compared with other orientations, discussions based on the atomic orbital are partially still valid. For example, as the width of NWs becomes thicker under a constant height, the amount of contribution from p orbitals along the width direction increases, as shown in Fig. 3. We suppose that this is because the p-orbital state along the weaker confinement direction has smaller energy shift. It should be also pointed out that the VBM state of [001] NWs has larger energy shift than that of [110] and [111] NWs (see Figs. 4,7, and 10). This may be due to the incorporation of transverse p states to the VBM state of [001] NWs.

V. CONCLUSIONS

To investigate the effects of quantum confinement on hole states in silicon nanowires, the valence band structure, hole effective mass, and wave function of hole states of [001], [110], and [111] oriented rectangular cross-sectional Si NWs have been studied using an $sp^3d^5s^*$ tight-binding method. We summarize the insights obtained by this study following. (i) By atomic orbital analyses, it was found that three p atomiclike orbitals oriented to length, height, and width axes of nanowires well describe the valence states of Si NWs. (ii) The hole states with larger composition of the axially-oriented p orbital show smaller transport effective mass, and those with larger composition of the p orbital oriented toward the confinement direction exhibit larger negative energy shift by quantum confinement. These results are understandable by considering the amount of overlap of orbitals between neighbor atoms. (iii) In [110] and [111] NWs, the axially-oriented orbitals are well separated from the others, and thus different types of subbands with small effective mass and large effective mass appear. Since the p orbital along the transport direction exhibit smaller overlap of orbitals toward the confinement direction than other orbitals, the subbands with light effective mass have smaller energy shift by quantum confinement than those with heavy effective mass and thus the valence band maximum is formed by the subband with light effective mass. (iv) The heavy band of [110] NWs has strong anisotropy regarding confinement-induced energy shift (sensitive to $[1\bar{1}0]$ confinement, but insensitive to [001]). However, the heavy band of [111] NWs does not have such anisotropy. This difference is caused by the fact that the heavy band in [110] NWs is formed by single p orbital along $[1\bar{1}0]$ but that in [111] NWs is formed by two p orbitals along confinement directions. (v) The hole states in [110] and [111] NWs seems to have a relationship to bulk hole state in the limit of weak SO coupling. The effective mass of the light subband in [110] and [111] NWs obtained by our calculation is very close to that of the bulk light-hole state and insensitive to the variation of NW size. Comparing the wave function of the bulk (without spin-orbit coupling), the orbital character of nanowires and bulk is very similar, which indicates the close relationship between NWs' light band and bulk's light-hole state. Moreover, the heavy subband states in [110] and [111] NWs have similar character as the bulk heavy-hole state. (vi) The topmost valence state of [001] NWs is formed by the mixture of the three characters of p orbitals in contrast to other orientations. Because the mixture fraction of orbitals changes by the variation of the width and height, the effective mass of [001] wire is sensitive to the wire dimension and geometry.

ACKNOWLEDGMENTS

This work was supported by the Global COE Program (C09) from the Ministry of Education, Culture, Sports, Science and Technology, Japan.

[1] A. G. Nassiopoulos, S. Grigoropoulos, and D. Papadimitriou, Appl. Phys. Lett. **69**, 2267 (1996).
[2] J. D. Holmes, K. P. Johnston, R. C. Doty, and B. A. Korgel, Science **287**, 1471 (2000).
[3] "Internaional Technology Roadmap for Semiconductors 2009" (2009), http://www.itrs.net/.
[4] S. Miyano, M. Hirose, and F. Masuoka, IEEE Trans. Electron Devices **39**, 1876 (1992).
[5] E. Leobandung, J. Vac. Sci. Technol. B **15**, 2791 (1997).
[6] C. Auth and J. Plummer, IEEE Electron Device Lett. **18**, 74 (1997).
[7] T. Saito, T. Saraya, T. Inukai, H. Majima, T. Nagumo, and T. Hiramoto, IEICE Trans. Electronics **E85-C**, 1073 (2002).
[8] J.-T. Park and J.-P. Colinge, IEEE Trans. Electron Devices **49**, 2222 (2002).
[9] N. Singh, A. Agarwal, L. Bera, T. Liow, R. Yang, S. Rustagi, C. Tung, R. Kumar, G. Lo, N. Balasubramanian, and D. Kwong, IEEE Electron Device Lett. **27**, 383 (2006).
[10] Y. Cui, Z. Zhong, D. Wang, W. U. Wang, and C. M. Lieber, Nano Lett. **3**, 149 (2003).
[11] J. Chen, T. Saraya, and T. Hiramoto, in *2010 Symposium on VLSI Technology Digest of Technical Papers* (2010), pp. 175–176.
[12] A. B. Filonov, G. V. Petrov, V. A. Novikov, and V. E. Borisenko, Appl. Phys. Lett. **67**, 1090 (1995).
[13] T. Vo, A. J. Williamson, and G. Galli, Phys. Rev. B **74**, 045116 (2006).
[14] J. A. Yan, L. Yang, and M. Y. Chou, Phys. Rev. B **76**, 115319 (2007).
[15] J. Wang, A. Rahman, G. Klimeck, and M. S. Lundstrom, in *Tech. Digest of IEEE Int. Electron Device Meeting* 2005 (2005), pp. 530–533.
[16] Y. Zheng, C. Rivas, R. Lake, K. Alam, T. B. Boykin, and G. Klimeck, IEEE Trans. Electron Devices, **52**, 1097 (2005).
[17] K. Nehari, N. Cavassilas, J. L. Autran, M. Bescond, D. Munteanu, and M. Lannoo, Solid-State Electron. **50**, 716 (2006).
[18] C. Harris and E. P. O'Reilly, Physica E **32**, 341 (2006).
[19] N. Neophytou, A. Paul, M. S. Lundstrom, and G. Klimeck, IEEE Trans. Electron Devices **55**, 1286 (2008).
[20] N. Neophytou, A. Paul, and G. Klimeck, IEEE Trans. Nanotechnol. **7**, 710 (2008).
[21] D. Karanth and H. Fu, Phy. Rev. B **74**, 155312 (2006).
[22] B. Lassen, M. Willatzen, R. Melnik, and L. C. Lew Yan Voon, J. Mater. Res. **21**, 2927 (2006).
[23] J.-M. Jancu, R. Scholz, F. Beltram, and F. Bassani, Phys. Rev. B **57**, 6493 (1998).
[24] J. C. Slater and G. F. Koster, Phys. Rev. **94**, 1498 (1954).
[25] T. B. Boykin, G. Klimeck, and F. Oyafuso, Phys. Rev. B **69**, 115201 (2004).
[26] D. J. Chadi, Phys. Rev. B **16**, 790 (1977).
[27] S. Lee, F. Oyafuso, P. von Allmen, and G. Klimeck, Phys. Rev. B **69**, 045316 (2004).
[28] P.-O. Löwdin, J. Chem. Phys. **18**, 365 (1950).
[29] O. Madelung, ed., *Group IV Elements and III–V Compounds* (Springer, Berlin, 1991).
[30] N. Neophytou and G. Klimeck, Nano Lett. **9**, 623 (2009).
[31] P. W. Leu, A. Svizhenko, and K. Cho, Phys. Rev. B **77**, 235305 (2008).

[32]D. Shiri, Y. Kong, A. Buin, and M. P. Anantram, Appl. Phys. Lett. **93**, 073114 (2008).
[33]X.-H. Peng, A. Alizadeh, S. K. Kumar, and S. K. Nayak, Int. J. Appl. Mech. **01**, 483 (2009).
[34]A. N. Kholod, V. L. Shaposhnikov, N. Sobolev, V. E. Borisenko, F. A. D'Avitaya, and S. Ossicini, Phys. Rev. B **70**, 035317 (2004).
[35]P. Logan and X. Peng, Phys. Rev. B **80**, 115322 (2009).
[36]Y. M. Niquet, A. Lherbier, N. H. Quang, M. V. Fernàndez-Serra, X. Blase, and C. Delerue, Phys. Rev. B **73**, 165319 (2006).
[37]M. P. Persson and H. Q. Xu, Appl. Phys. Lett. **81**, 1309 (2002).
[38]T. B. Boykin, Phys. Rev. B **52**, 16317 (1995).
[39]G. Dresselhaus, A. F. Kip, and C. Kittel, Phys. Rev. **98**, 368 (1955).
[40]N. Neophytou, S. G. Kim, G. Klimeck, and H. Kosina, J. Appl. Phys. **107**, 113701 (2010).